International Journal of Sciences: Basic and Applied Research (IJSBAR)

ISSN 2307-4531
(Print & Online)

http://gssrr.org/index.php?journal=JournalOfBasicAndApplied

Determination of Far-Field Pattern Expressions for Helical Antenna Analyzed Using Curved Segments Moment Method

Abderrahmane Badis*

Electrical and Electronic Communication Engineer from UMBB (Ex.INELEC), Independent Electronics, Aeronautics, Propulsion, Well Logging and Software Design Research Engineer, Takerboust, Aghbalou, Bouira 10007, Algeria

Email: Badis.dahmane@gmail.com

Abstract

The use of moment method with curved segments for numerically modeling helical antennas has been the scope of many papers, it is mainly used to solve for the current distribution on the helix contour with high accuracy at a reduced number of segments. It is often very challenging to use the resulting electrical current distribution to evaluate the far field expressions. This paper is intended to cover the development of the far field expressions for a helix antenna analyzed using moment method under curved basis and testing functions. The electric field is expressed in unified expressions based on the antenna current distribution. The validity of the obtained expressions is verified through the analysis of commonly known operation modes by choosing different geometries for the Helical Antenna.

Keywords: Helical Antenna; Far-Field Pattern; Moment Method; Curved Segments.

---

* Corresponding author.

1. Introduction

The helical antenna is a hybrid of two simple radiating elements, the dipole and loop antenna. A helix is considered as linear antenna when its diameter approaches zero [1]. On the other hand, a helix of fixed diameter is seen as a loop antenna when the spacing between the turns vanishes. Helical antennas have been widely used as simple and practical radiators over the last decades thanks to their notable properties including their circular polarization, high gain, wide bandwidth and simplicity of construction.

Although many radiation patterns are possible, two kinds are of particular interest:

- The Normal Mode in which the maximum radiation occurs in the plane perpendicular to the helix axis. In this mode, the helix is used without ground plane.
- The Axial Mode in which the radiation occurs in the direction of its axis. In this mode, the helix is usually backed by a ground plane.

Unlike the dipole and loop antennas whose characteristics are well defined, the helix and because of its complicated geometry, has no exact solutions that describe its performance. To overcome this limitation, experimental approaches and approximate analytical methods [2-4] are instead used. In the present work, an attempt is made to complement the full wave analysis technique based on curved segments moment method toward the determination of the radiated far-field patterns based on the resulting curvilinear current distribution.

2. Basic Helix Antenna Geometry

A helix is a basic 3-dimentional shape that combines the geometric forms of a straight line, a circle and a cylinder. In addition a helix has handedness; it can be either left- or right-handed. Figure 1 shows the basic geometry of helical antenna. The defining parameters of the conventional helix are the helix diameter D = 2 x ρ , the helix conductor diameter d = 2 x a, the helix circumference C, the turn-to-turn spacing S, the pitch angle of the turns α, and the axial length A = n × S. In addition some other parameters are often used such as the length of 1 turn L, and the total number of turns N. The diameter D and the circumference C of an imaginary cylinder whose surface passes through the centerline of the helix conductor.

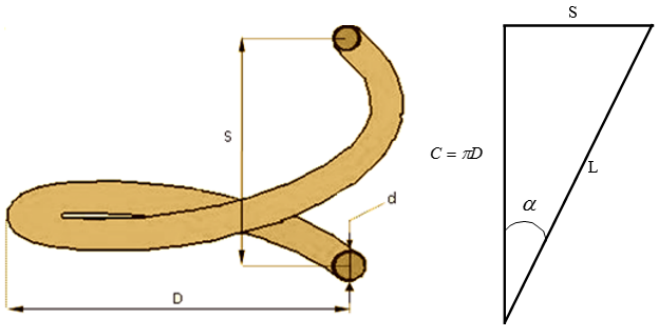

Figure 1: Basic Helix Geometry

3. Helix Antenna Analysis Using Curved Segments Moment Method

The Moment Method (MoM) [5] is a powerful technique used to solve linear equations, it is a highly accurate and adaptable tool for antenna analysis. The MoM is used to convert the antenna electric field integral equation into a matrix system of linear equations, which could be then solved for the current coefficients by LU decomposition, Gaussian elimination, or any other techniques of linear Algebra.

The helix geometry configuration illustrated in Figure 2 has been adopted for the analysis. The helix is oriented along the z-axis, perpendicular to the xy-plane. In addition to the previously described parameters, z_0 is the helix xy-plane distance and $\hat{\ell}$ is the tangential unit vector describing the contour of the helix.

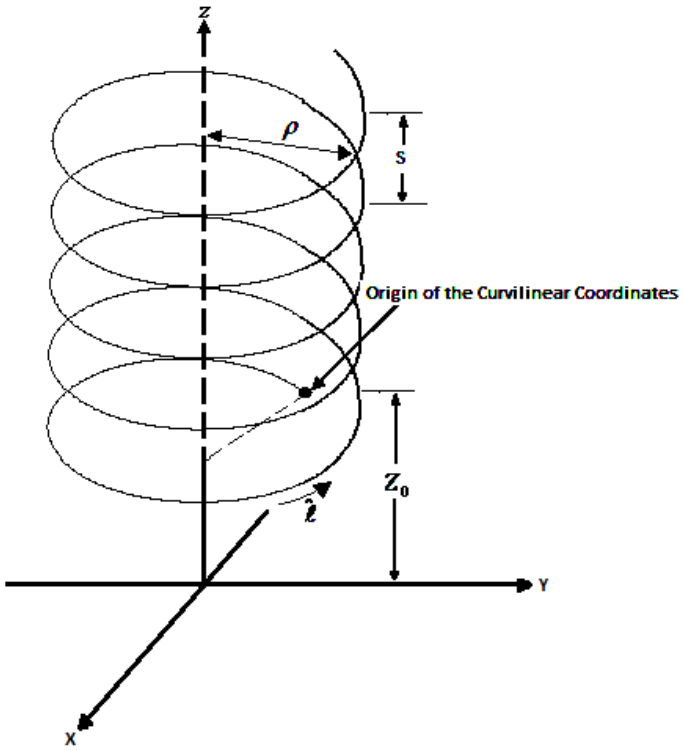

Figure 2: Helix Antenna Geometrical Structure

The relation between the current on the Helix contour to the incident electric field is derived by adapting the generalized Electric Field Integral Equation (EFIE) to the helix structure illustrated in Figure 2 [6].

$$\hat{\ell}' \cdot \frac{j}{\omega \varepsilon_0} \int_{\ell'} \left[\hat{\ell}' k^2 I(\ell') G(R) + \left(\frac{\partial}{\partial \ell'} I(\ell') \right) \nabla G(R) \right] d\ell' = \hat{\ell} \cdot \vec{E}_i \qquad (1)$$

Where $\hat{\ell}$ and $\hat{\ell}'$ denote tangent unit vectors at the observation point and at the source point, respectively. R is the distance between the source and the observation point. G is the free space Green's Function.

The application of the Moment Method to Integral Equation (1) [6] by approximating the current as a sum of basis function $I(\ell') = \sum_n I_n u_n(\ell')$ and introducing the weighting functions presented by $w_n(\ell)$ yields

$$\frac{j}{\omega\varepsilon_0}\sum_n I_n\left[k^2\int_\ell w_m(\ell)\int_{\ell'}(\hat{\ell}\cdot\hat{\ell}')u_n(\ell')G(R)d\ell' d\ell + \int_\ell w_m(\ell)\frac{\partial}{\partial\ell}\int_{\ell'}G(R)\frac{\partial}{\partial\ell'}u_n(\ell')d\ell' d\ell = \int_\ell w_m(\ell)\hat{\ell}\cdot\vec{E}_i d\ell\right] \quad (2)$$

In this work, the basis and weighting functions are chosen as two segment wide triangles centered about the junction between two segments and the weighting functions are one-segment pulses centered about the junction. For the feed excitation, the delta-gap source model is used.

It is worth mentioning that the accuracy of the Integral Equation (2) is very dependent on the arc segments lengths with their corresponding unit vectors (number of segments used). The impedance matrix [Z] which relates the current and the electric field in the gap is obtained by the rearrangement of the Integral Equation (2) which implies to a linear equation in the form [Z] [I] = [V]. This equation may be easily solved to get the current through $[I] = [Z]^{-1}[V]$. The Romberg numerical integration method is used, in which the composite trapezoidal rule approximations are linearly combined using the Richardson extrapolation to get an adequate approximation of the integral.

If the Helix is operated in the Axial Mode, a ground plane will be backing the antenna on the xy-plane, then the image theory is used. In this case, an image antenna below the ground plane is introduced and then the ground plane is removed. The resulting moment method impedance matrix is given by $Z = Z_{Real} + Z_{Image}$ which reflects the effect of the real and the image currents.

The reader is invited to get through the work presented by [6] for more details on the application of the curved segments Moment Method on helical antenna. This paper is mainly intended to derive the electric far-field expressions that describes the radiation patterns based on the curvilinear currents obtained using this approach.

4. Determination of the Electric Far-Field Radiation Pattern

The antenna radiation Pattern is a graphical representation of the antenna radiation properties as a function of position. One common type of patterns is the field pattern, in which a normalized electric or magnetic fields are presented on a spherical coordinates system.

Once the current distribution is obtained, the radiation field may be found. This section is devoted to the derivation of the electric far-field expressions. To accomplish this, the general electric far-field equation [7] given below is used

$$\vec{E}(M) = j\frac{k}{4\pi}\psi(r)\cdot\int_{v'}\left\{\eta\left(\vec{J}\times\hat{r}\right)-\vec{J}_m\right\}\times\hat{r}e^{jk\hat{r}\cdot\vec{r}'}dv' \quad (3)$$

Where $\vec{E}(M)$ is the electric far-field victor at point M, the function $\psi(r)=\frac{e^{-jkr}}{r}$, η is the wave impedance defined as $\eta=\sqrt{\frac{\mu}{\varepsilon}}$, k is the wave number define as $k=\omega\sqrt{\varepsilon\ \mu}$ with μ and ε being the permeability and permittivity of the medium, $\vec{J}$ and $\vec{J}_m$ are the electric and magnetic current densities respectively.

The Observation point unit victor $\hat{r}$ is spherical radial unit vector defined in rectangular coordinates as

$$\hat{r}=\hat{x}\sin\theta\cos\phi+\hat{y}\sin\theta\sin\phi+\hat{z}\cos\theta \quad (4)$$

The sources position vector $\vec{r}'$ is defined as

$$\vec{r}'=\hat{x}\rho\cos\left(\frac{2\pi}{L}\ell'\right)+\hat{y}\rho\sin\left(\frac{2\pi}{L}\ell'\right)+\hat{z}\left(\ell'\sin\alpha+z_0\right) \quad (5)$$

By introducing the thin wire approximation (i.e. $\vec{J}=I(\ell')\hat{\ell}$) and since no magnetic sources exist $\vec{J}_m=0$ with η being a constant, Equation (3) can be written in the form

$$\vec{E}(M)=j\frac{k\eta}{4\pi}\psi(r)\cdot\int_{\ell'}\left(\vec{J}\times\hat{r}\right)\times\hat{r}e^{jk\hat{r}\cdot\vec{r}'}d\ell' \quad (6)$$

The replacement of the current $I\left(\ell'\right)$ defined above in Equation (6) results

$$\vec{E}(M)=j\frac{k\eta}{4\pi}\psi(r)\cdot\sum_n\left[I_n\int_{\ell'}u_n(\ell')\left(\hat{\ell}\times\hat{r}\right)\times\hat{r}\,e^{jk\hat{r}\cdot\vec{r}'}d\ell'\right] \quad (7)$$

Where the unit victor $\hat{\ell}'$ which describes the helix to observation point is given by

$$\hat{\ell}'=-\hat{x}\cos\alpha\cos\left(\frac{2\pi}{L}\ell'\right)+\hat{y}\cos\alpha\sin\left(\frac{2\pi}{L}\ell'\right)+\hat{z}\sin\alpha \quad (8)$$

Evaluation of the field given in Equation (7) requires the expansion of the two vector operations within the integral.

$$\vec{r}'\cdot\hat{r} = X\cos\left(\frac{2\pi}{L}\ell'\right) + Y\sin\left(\frac{2\pi}{L}\ell'\right) + Z\ell' + z_0\cos\theta \tag{9}$$

With $X = \rho\sin\theta\cos\phi$, $Y = \rho\sin\theta\sin\phi$ and $Z = \cos\theta\sin\alpha$.

The vector operation $(\hat{\ell}'\times\hat{r})\times\hat{r}$ is evaluated and written in spherical coordinates as

$$(\hat{\ell}'\times\hat{r})\times\hat{r} = [-A\cos\theta\cos\phi - B\cos\theta\sin\phi + C\sin\theta]\hat{\theta} + [A\sin\phi - B\cos\phi]\hat{\phi} \tag{10}$$

With $A = -\cos\alpha\sin\left(\frac{2\pi}{L}\ell'\right)$, $B = \cos\alpha\cos\left(\frac{2\pi}{L}\ell'\right)$ and $C = \sin\alpha$.

Thus, the electric far-field expressions are

$$E_\theta = j\frac{k\eta}{4\pi}\psi(r)\sum_n I_n\int_{\ell'} u_n(\ell')\cdot\left(-A\cos\theta\cos\phi - B\cos\theta\sin\phi + \sin\alpha\sin\theta\right)\cdot e^{jk\hat{r}\cdot\vec{r}'}d\ell' \tag{11}$$

$$E_\phi = j\frac{k\eta}{4\pi}\psi(r)\sum_n I_n\int_{\ell'} u_n(\ell')\cdot\left(A\sin\phi - B\cos\theta\right)\cdot e^{jk\hat{r}\cdot\vec{r}'}d\ell' \tag{12}$$

Notes:

- The transformation from Cartesian Coordinates to Spherical Coordinates shows clearly that the radiated electrical far-field has only two components $\vec{E}_\theta$ and $\vec{E}_\phi$.
- The Term $z_0\cos\theta$ in Equation (9) could be neglected as the dimension of z_0 is often very small compared to wavelength.
- The same approach could be used to derive the Magnetic Far-Field radiation pattern using the general magnetic far-field equation [7] given below

$$\vec{H}(M) = j\frac{k}{4\pi}\psi(r)\cdot\int_{v'}\left\{\frac{1}{\eta}\left(\vec{J}_m\times\hat{r}\right) + \vec{J}\right\}\times\hat{r}e^{jk\hat{r}\cdot\vec{r}'}dv' \tag{13}$$

- Normalized or relative field patterns are used, this done through dividing field components described by Equations (11) and (12) by their maximum values to obtain dimensionless values with maximum of unity.

5. Application of the Far-Field Expressions

The developed Integral Equations to solve for the impedance matrix are implemented under C++ Code. The

obtained impedance matrix is saved in a data file that is used by a MATLAB program to compute the current distribution and to plot the normalized electric far-field patterns for the considered helix configuration.

5.1. Approximation of a 0.47λ Length Dipole

A helix antenna reduces to straight wire structure when the pitch angle α equals 90°. The discussed method cannot check for exactly 90° as the length of one turn blows up ($L = \frac{2\pi\rho}{\cos\alpha}$). As such the simulation has been performed for a pitch angle of 89°. The antenna has been broken to 24 segments. The helix is without any ground plane and was center fed. The parameters of the helix approximating a dipole of 0.47λ are given in the Table 1.

Table 1: Helix Approximating a 0.47λ Dipole

Helix Parameters	Numerical Values
Helix radius(ρ)	0.02 λ
Pitch angle (α)	89°
Number of turns (N)	0.06527
Wire radius (a)	0.005 λ

Figure 3 shows the obtained current distribution and Figure 4 the associated normalized patterns for the theta component, the phi component and the total field. All the fields are plotted in the $\phi = 0$ plane. As expected, the radiation patterns obtained for dipole antenna contain only two principal lobes as indicted in the figures. The maximum radiation is in the vertical directions to the dipole corresponding to $\theta = 0$ and $\theta = \pi$. The nulls are in the horizontal directions corresponding to $\theta = \frac{\pi}{2}$ and $\theta = \frac{3\pi}{2}$.

The data shows that the helix approximation give practically the same results as a resonant 0.47λ Length Dipole. The radiation patterns matches well those of a dipole antenna. The proposed Far-Field expressions are verified through this special case for the helix in free space.

5.2. Normal Mode Helix

The parameters used to analyze the normal mode helix are summarized in Table 2. The helix has a height of 0.2 λ and a total wire length of 0.774 λ. The helix is without any ground plane and was center fed. Figure 5 and 6 show the obtained current distribution and the radiation patterns respectively using 20 segments.

Notice that the current distribution for the normal mode is sinusoidal in shape and has an even symmetry about the center of the helix.

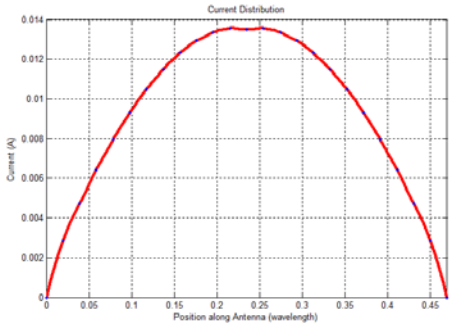

Figure 3: Current Distribution for a Helix Approximating of a 0.47λ Length Dipole

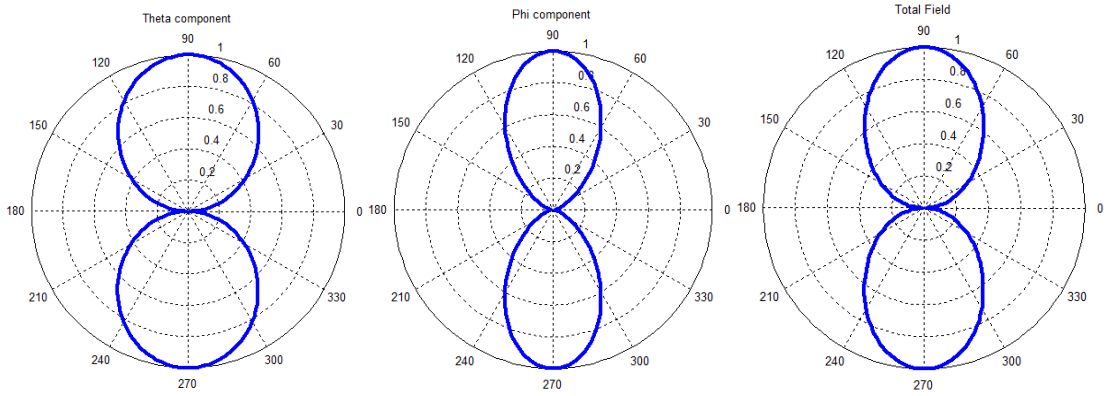

Figure 4: Normalized Far-Field Radiation Patterns for a Helix Approximating of a 0.47λ Length Dipole

Table 2: Normal Mode Helix Parameters

Helix Parameters	Numerical Values
Helix radius(ρ)	0.007λ
Pitch angle (α)	15°
Number of turns (N)	17
Wire radius (a)	0.0007 λ

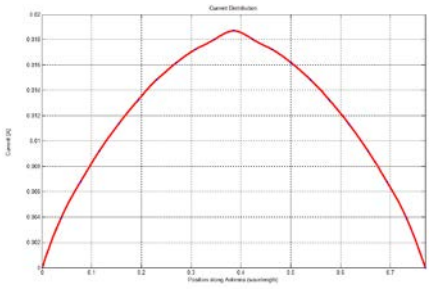

Figure 5: Current Distribution for a Normal Mode Helix

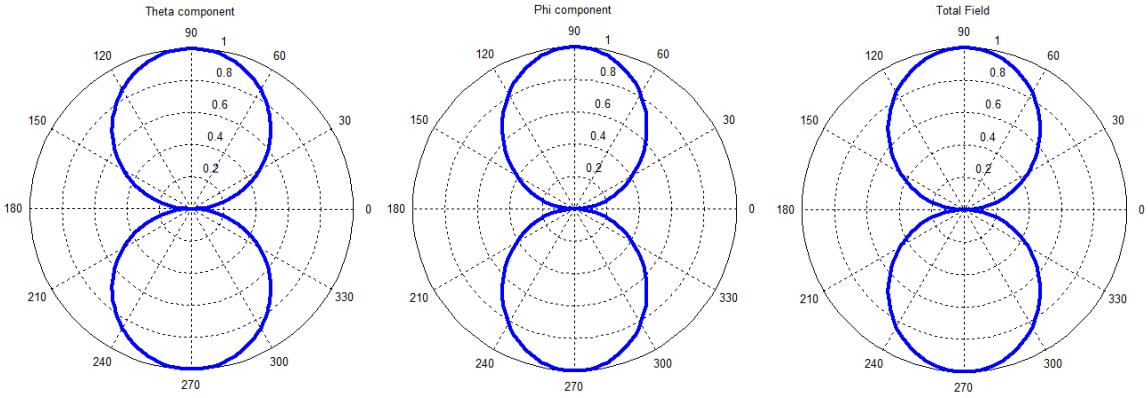

Figure 6: Normalized Far-Field Radiation Patterns for a Normal Mode Helix

The radiation patterns obtained for the normal mode helix contain only two principal lobes with maximums in the vertical directions to the helix corresponding to $\theta = 0$ and $\theta = \pi$.

The nulls are in the horizontal directions corresponding to $\theta = \frac{\pi}{2}$ and $\theta = \frac{3\pi}{2}$.The radiation pattern does not have any side lobes because the normal mode helix dimensions are very small compared to the wavelength.

5.3. Axial Mode Helix

Some distinguishing practical considerations of the axial mode helix are implemented; the helix is backed by a ground plane and it is peripherally fed.

The parameters of the analyzed helix are summarized in Table 3. The helix radius is chosen such that the circumference of one turn equals one wavelength.

Figure 7 and 8 show the obtained current distribution and the radiation patterns respectively using 50 segments.

The current magnitude shows an initial decay of current from the feed-point. This is followed by a slight increase in magnitude, which then settles down to gradual rippling decay. At the end of the helix, we notice a region of small standing waves.

This is the result of interaction between forward and reverse traveling waves. The decay at the input end could be understood as a transition between a helix-to-ground-plane.

All field Patterns are plotted in the $\phi = 0$ plane, they consist of principal lobs in the horizontal direction corresponding to $\theta = \frac{\pi}{2}$. The appearance of side lobes is due to the fact that the axial mode helix dimensions are greater than the wavelength.

Table 3: Axial Mode Helix Parameters

Helix Parameters	Numerical Values
Helix radius(ρ)	0.159λ
Pitch angle (α)	13°
Number of turns (N)	10
Wire radius (a)	0.005 λ

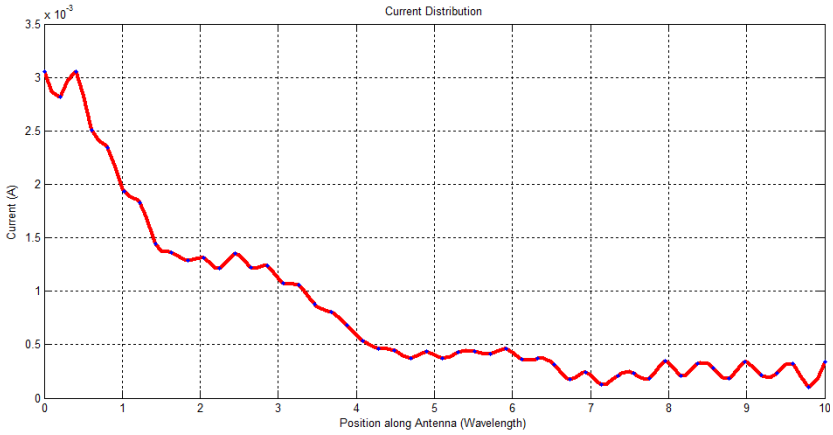

Figure 7: Current Distribution for an Axial Mode Helix

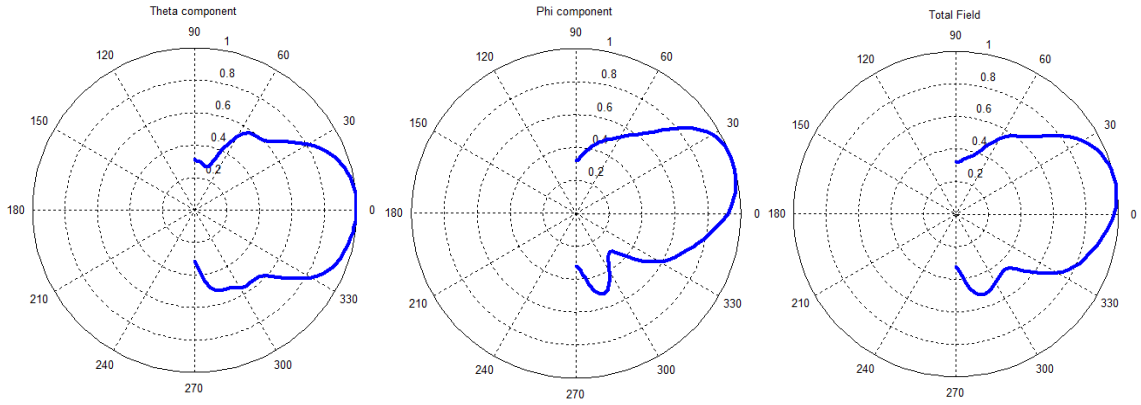

Figure 8: Normalized Far-Field Radiation Patterns for an Axial Mode Helix

6. Conclusion

This paper presented a flexible technique to plot the far-field pattern for a helical antenna structure analyzed using moment method based on curved segments. The developed expressions uses the resulting electrical current distribution in a unified equations to evaluate the Theta and Phi component of the radiated electrical far-field. The obtained radiated fields are validated through the analysis of an approximated 0.47λ Length Dipole and the analysis of the helix antenna normal and axial modes.

Prospective future work exists; expressions for the magnetic field component could be derived based on the

same demonstration. The derived expressions could be used to analyze other helix modes of operations. The increase of the number segments will also increase the accuracy of the results. Expressions for other more complicated structures helices, wires and curved surfaces could be derived based on the same approach.

Acknowledgment

The author acknowledges Dr. Arab AZRAR from the Institute of Electrical and Electronic Engineering in Boumerdès Algeria for providing help and support.

References

[1] J. D. Kraus, “Antennas”, 2nd editor, McGraw Hill, New York, 1988.

[2] H. E. King and J. L. Wong, “Characteristics of 1 to 8 wavelength uniform helical antennas,” IEEE trans. Antennas Propagat., vol. AP-28, No. 2, pp. 291-296, March 1980.

[3] D. T. Emerson, “The gain of the axial-mode helix antenna,” Antenna Compendium, vol. 4, pp. 64-68, 1995.

[4] W. L. Stutzman, and G. A. Thiele, “Antenna Theory and Design”, John Wiley & Sons, New York, 1981.

[5] R. F Harrington, “Field Computation by Moment Methods”, New-York 1968.

[6] Eric Caswell, "Analysis of a Helix Antenna Using a Moment Method Approach With Curved Basis and Testing Functions", M. &.Thesis, Virginia Polytechnic Institute, 1998.

[7] C. A. Balanis, "Antenna Theory: Analysis and Design", 3rd Edition, John Wiley & Sons, New York, Chapter 3, 2005.